Environ Monit Assess (2018) 190: 341
https://doi.org/10.1007/s10661-018-6712-5

Determining $\delta^{15}N-NO_3^-$ values in soil, water, and air samples by chemical methods

Chaopu Ti · Xi Wang · Xiaoyuan Yan

Received: 5 October 2017 / Accepted: 2 May 2018 / Published online: 10 May 2018

Abstract Soil, water, and air NO_3^- pollution is a major environmental problem worldwide. Stable isotope analysis can assess the origin of NO_x because different NO_x sources carry different isotope signatures. Hence, using appropriate chemical methods to determine the $\delta^{15}N-NO_x$ values in different samples is important to improve our understanding of the $N-NO_x$ pollution and take possible strategies to manage it. Two modified chemical methods, the cadmium–sodium azide method and the VCl_3–sodium azide method, were used to establish a comprehensive inventory of $\delta^{15}N-NO_x$ values associated with major NO_x fluxes by the conversion of NO_3^- into N_2O. Precision and limit of detection values demonstrated the robustness of these quantitative techniques for measuring $\delta^{15}N-NO_x$. The standard deviations of the $\delta^{15}N-NO_3^-$ values were 0.35 and 0.34‰ for the cadmium–sodium azide and VCl_3–sodium azide methods. The mean $\delta^{15}N-NO_3^-$ values of river water, soil extracts, and summer rain were 8.9 ± 3.3, 3.5 ± 3.5, and 3.3 ± 2.1‰, respectively. The $\delta^{15}N-NO_3^-$ values of low concentration samples collected from coal-fired power plants, motor vehicles, and gaseous HNO_3 was 20.3 ± 4.3, 5.6 ± 2.78, and 5.7 ± 3.6‰, respectively. There was a good correlation between the $\delta^{15}N-NO_3^-$ compositions of standards and samples, which demonstrates that these chemical reactions can be used successfully to assess $\delta^{15}N-NO_3^-$ values in the environment.

Keywords Environmental $\delta^{15}N-NO_3^-$ · Chemical method · PT-IRMS · Source identification

Introduction

Nitrogen (N) is a key nutrient, essential to the survival of humans and all other living organisms. However, the generation of reactive N by humans has at least doubled the rate of input of reactive N to the earth system. The release of a large amount of N will overcome several thresholds set for the health of humans and the ecosystem, including those for drinking water pollution, air quality degradation, freshwater eutrophication, biodiversity loss, stratospheric ozone depletion, and climate change (Erisman et al. 2013). One of the major species of fixed N is NO_3^--N, mainly from atmospheric deposition, sewage NO_3 discharge, and NO_3 fertilizer application (Kendall et al. 2007; Michalski et al. 2004). Therefore, understanding the origin of NO_3^--N is critical to implement possible strategies for managing the N pollution problem.

Isotope analysis is a methodology used worldwide to assess the cycle of N through the environment because N-rich sources carry different stable isotope signatures (Hastings et al. 2013). For example, $\delta^{15}N$ values of NO_3^- from organic fertilizers display typical values ranging from − 6 to 6‰, whereas $\delta^{15}N$ values

---

Chaopu Ti and Xi Wang contributed equally to this work.

C. Ti · X. Wang · X. Yan (✉)
State Key Laboratory of Soil and Sustainable Agriculture, Institute of Soil Science, Chinese Academy of Sciences, 71 East Beijing Road, Nanjing 210008, People's Republic of China
e-mail: yanxy@issas.ac.cn

of atmospheric N depositions are between − 13 and 13‰. In addition, $\delta^{15}N$ values of soil and surface groundwater have been shown to range from 0 to 8 and − 4 to 15‰, respectively (Kendall 1998; Mayer et al. 2002; Xue et al. 2009). Furthermore, $\delta^{15}N$ values of NO_x generated from natural sources are always lower than those generated by anthropogenic sources (Felix and Elliott 2014; Freyer 1978). Previous studies characterizing the $\delta^{15}N$ composition of NO_x emissions from power plants (− 9–26‰) have shown that that these are important NO_x sources driving the deposition of NO_3^- at rural monitoring sites in the eastern USA (Elliott et al. 2007; Felix et al. 2012). Stable N isotope data of NO_3^- ($\delta^{15}N$-NO_3^-) can be used to trace the production and destination of NO_3^--N. Thus, precise and accurate, but also inexpensive and rapid, $\delta^{15}N$-NO_3^- analyses are needed to improve the identification and assessment of NO_3^- in atmospheric, soil, surface water, and groundwater samples and samples from their emission sources. During the past decades, a variety of analytical methods have been developed to determine $\delta^{15}N$ in NO_3^-, such as ion exchange and bacterial denitrification (Casciotti et al. 2002; Rock and Ellen 2007; Sigman et al. 2001; Xue et al. 2010). However, these methods have some associated drawbacks; e.g., Silva et al. (2000) pointed out that ion exchange or the $AgNO_3^-$ method is relatively labor intensive, requires a large volume of sample (sample size of 100–200 mmol of NO_3^-), and is time-consuming (3–5 days for sample preparation). The bacterial denitrification method also requires a long time for bacterial growth, as long as 10–12 days from Petri dish to media bottles (Xue et al. 2009). A series of chemical methods for $\delta^{15}N$-NO_3^- analysis have been created for sea water, freshwater, and soil samples. These approaches can analyze samples with low volume, and concentrations of samples do not produce interferences at high concentrations and also have the potential to be less labor-intensive than other approaches (Braman and Hendrix 1989; Lachouani et al. 2010; Tsunogai et al. 2008).

Compositions of $\delta^{15}N$-NO_3^- can provide evidence of the NO_3^--N sources and the mechanisms of NO_3^--N transformations in terrestrial ecosystems. Although recent methods used to analyze $\delta^{15}N$-NO_3^- in surface water and soil are advanced, it is necessary to analyze $\delta^{15}N$-NO_3^- in other samples, such as $\delta^{15}N$-NO_3^- in NO_x-N samples emitted from coal-fired plants and vehicles, which are absorbed by strong acid, alkali, or oxidant solutions. In addition, the chemical method is a new technique to measure $\delta^{15}N$-NO_3^-; therefore, it requires further demonstration.

Here, we present a series of chemical methods for detecting sensitive natural abundance of $\delta^{15}N$-NO_3^- in surface water, rainfall, soil, air, and coal-fired power plant and vehicular emission samples. The objectives of this study were as follows: (1) to develop improved chemical methods to determine the $\delta^{15}N$-NO_3^- composition of low-concentration samples with small volumes and complex absorbing solutions and (2) to identify the $\delta^{15}N$-NO_3^- signatures of NO_3^--N at environmental concentrations.

Materials and methods

Collection of NO_3^--N in river, rain, and soil

The collection of water samples (river and rain water) were conducted at Suzhou in southeast China during summer (June–August 2014). River water samples were collected in the central stream using a polyethylene barrel at a depth of 0.5 to 1 m from the water surface. Rain water samples were collected by a sensor-controlled auto sampler (ZJC-II, Zhejiang Hengda Instrument Company, China), which collected samples during precipitation events. All samples were subsequently transferred into plastic bottles (0.2–10 L) and transported on ice to the laboratory for storage at − 5 °C prior to analysis.

Soil samples were collected from a summer rice–winter wheat rotated cropland near Suzhou after the wheat harvest in 2014, and they were extracted by 2 mol L^{-1} KCl solution according to a water:soil ratio of 5:1.

Collection of NO_x-N in the atmospheric environment

Gaseous HNO_3 and NO_x emissions from coal-fired power plants and vehicles were collected in the Taihu Lake region during 2014 summer by an integrated air sampler (ZC-Q0102, Zhejiang Hengda Instrument Company, China). The sampler was operated for 24 h and gathered the ambient air by two low-volume pumps (1 L min^{-1}). The air was passed through a filter train.

Gaseous HNO_3 was absorbed by 0.5 g NaOH in 50 mL of methanol (pH > 12) following the method of Adon et al. (2010), and NO_x emission from coal-fired plants was trapped by a 25-mL aliquot of absorbing solution (6 mL of H_2O_2 in 1 L of ~0.05 M H_2SO_4) following the method of Felix et al. (2012). NO_x emissions from vehicles were absorbed in a tunnel (Jiuhua Tunnel, Nanjing City) by the same solution as the coal-fired power plant samples.

All the samples were stored at − 5 °C until required for further analysis. Previous studies have shown that the N isotopic fractionation resulting from the above conversions was minimal (Felix et al. 2012; Walters et al. 2015).

Analyses of NO_3^--N concentration

The water samples were filtered through glass fiber filters (Whatman, GF/F, 47 mm in diameter) and deposited in pre-cleaned polyethylene bottles. Samples collected from air and NO_x emission sources were adjusted to a pH of 8.0 by adding 1 mol L^{-1} hydroxide solution. The NO_3^--N concentrations in all of the collected samples were analyzed using a Skalar segmented flow-injection analyzer (Skalar San++ System, Breda, the Netherlands) with a relative error of ± 2% and a detection limit of 0.03 mg N L^{-1}.

Analyses of $\delta^{15}N$-NO_3^- in water and soil samples

Based on the methods of Stedman (1959a) and Stedman (1959b), McIlvin and Altabet (2005) developed a Cd reduction and N_3^- method to reduce NO_3^- in samples to N_2O for the determination of $\delta^{15}N$. In brief, in weak alkaline solution, cadmium reduces NO_3^- to NO_2^-, whereas NO_2^- reacts with N_3^- to produce N_2O in acidic conditions. The reaction between NO_2^- and N_3^- at a $pH > 2$ generates nitrous acidium ions ($H_2NO_2^+$), followed by the reaction with the N_3^-.

The resulting N isotopic composition of the N_2O product should be given by the mean of the the NO_3^- and N_3^- $\delta^{15}N$ values since each component contributes one N atom. Hence, we obtain Eq. (1):

$$\delta^{15}N_{Air}(N_2O) = \frac{\delta^{15}N_{Air}\left(N_3^-\right) + \delta^{15}N_{Air}\left(NO_2^-\right)}{2} = \frac{\delta^{15}N_{Air}\left(N_3^-\right) + \delta^{15}N_{Air}\left(NO_3^-\right)}{2} \tag{1}$$

The expected slope of a binary plot of NO_3^- standard $\delta^{15}N$ values versus the measured $\delta^{15}N$ of the produced N_2O is 0.5.

A graphical representation of the isotopic analysis method is given in Fig. 1.

We used a cadmium column to connect to a peristaltic pump, and the flow was set at 5 mL/min to perform the NO_3^- to NO_2^- reduction step. Furthermore, unlike the study of McIlvin and Altabet (2005), a pH of 8.0 was demonstrated to be optimal for the NO_3^- to NO_2^- conversion in our study (Fig. 2). Several drops of 0.5 M HCl were then added to decrease the pH to 2–3. Blanks require one drop of 0.5 M HCl to attain a pH of 3. The pH of blanks and samples were subsequently increased to 8.0 using a 1 M imidazole ($C_3H_4N_2$) solution. In cases in which too much imidazole was added, we added some drops of HCl to augment the pH again.

To convert NO_2^- to N_2O, we improved the methods developed by McIlvin and Altabet (2005) and Schilman and Teplyakov (2007). In brief, we poured 16 mL of sample remaining from the above procedure into a 50-mL headspace vial tightly capped with a Teflon-lined septum. The vial was put under vacuum and purged with He to eliminate the negative pressure effect. Then, 0.8 mL of N_3^- and acetic acid (CH_3COOH) buffer (15 mL of 2 mol L^{-1} N_3^- and 15 mL of 20% acetic acid) was added to vials via a syringe, and the vials were shaken vigorously for 1 min. According to McIlvin and Altabet (2005), the reaction must be kept at a pH between 4 and 5. All vials were put in a 30 °C water bath for 30 min. After 30-min quiescence, 0.5 mL of 6 M NaOH solution was injected into the vial with a syringe to produce a basic solution and stop the reaction. Afterwards, the pH of the reaction should be > 10. Three blanks were included in each sample batch to test the seals of the vial and the value of the reagent blank.

The vial's N_2O concentration was analyzed by an automated PT-IRMS which included a continuous flow IRMS (IsoPrime100, IsoPrime Limited, UK) with a cryo-focusing unit (Trace Gas Preconcentrator, IsoPrime Limited, UK). The sample entered the IRMS via a capillary from an open split directly to the ion source. Each sample was accompanied by a direct inlet injection of pure N_2O. Data were collected throughout the run for masses 44, 45, and 46. The area under each peak was calculated for each mass by Ionvantage software.

For the calculation of δ values, the δ notation is specified for a particular element *X*, where the

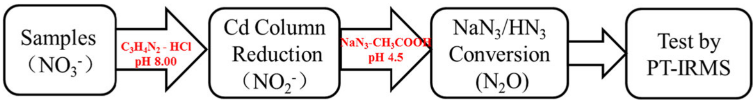

Fig. 1 Method schematic for the isotopic analysis of the isotopic analysis of δ^{15}N-NO_3^- by the cadmium–sodium azide method

superscript *H* gives the heavy isotope mass of that element,

$$\delta^H X = \left(\frac{R_{\text{sample}}}{R_{\text{standard}}} - 1\right) \tag{2}$$

where R_{sample} is the ratio of the heavy isotope to the light isotope of the sample and R_{standard} is the isotope ratio of the international standard (0.0036765). In this study, *R* was calculated by

$$R_{45}/_{44} = \frac{\text{area}_{45}}{\text{area}_{44}} \tag{3}$$

where area_{45} is the peak area of the *m*/*z* 45 of N_2O that contains a ^{15}N atom, while the area_{44} is the peak area of the *m*/*z* 44 of N_2O that does not contain a ^{15}N atom.

Analyses of δ^{15}N-NO_3^- in air samples

We can use the cadmium–sodium azide method to analyze the N natural isotopic abundance of freshwater and soil extracts, but this method is not suitable for samples absorbed with strong acid, alkali, or oxidant solutions because of the difficulty to adjust the pH in the cadmium–sodium azide process.

Therefore, we tried to use the chemical method defined by Lachouani et al. (2010) to determine the δ^{15}N-NO_x values for coal-fired power plant, motor vehicles, and gaseous HNO_3 samples those absorbed by strong acid, alkali, or oxidant solutions in this study.

The chemical reactions involved in this method are as follows:

$$NO_2 + NO + 3H_2O_2 \xrightarrow{H^+} 2NO_3^- + 3H_2O \tag{4a}$$

$$NO_3^- + 2V^{3+} + 2H^+ \rightarrow NO_2^- + 2V^{4+} + H_2O \tag{4b}$$

$$NO_2^- + 2H^+ \leftrightarrow H_2NO_2^+ \tag{4c}$$

$$H_2NO_2^+ + Cl^- \rightarrow NO{-}Cl + H_2O \tag{4d}$$

$$Cl{-}NO + N_3^- \xrightarrow{\text{fast}} N_3{-}NO + Cl^- \xrightarrow{\text{fast}} N_2 + N_2O \tag{4e}$$

The measured N_2O consists of two N atoms, one originating from the sample and the other from the sodium azide.

Fig. 2 Effects of pH on the reaction of NO_3^- to NO_2^- by the cadmium–sodium azide method

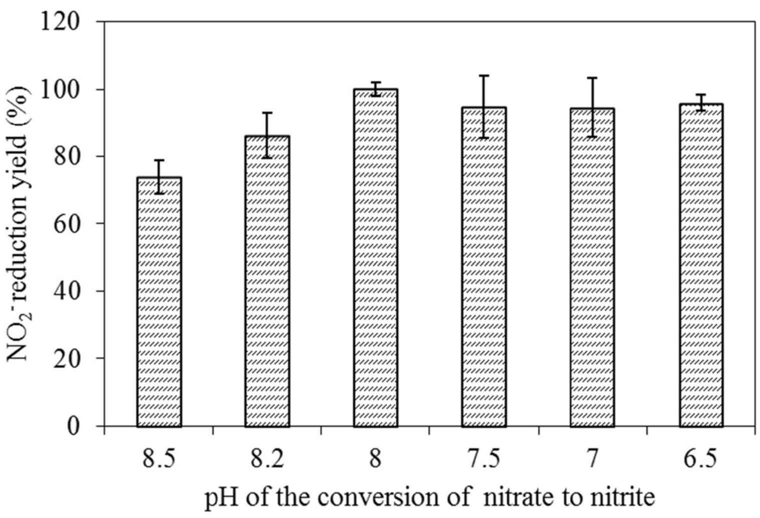

Lachouani et al. (2010) determined that the influence of blank $\delta^{15}N$ on the sample $\delta^{15}N$ composition should be corrected by the following mass balance equation:

$$\delta^{15}N_{\mathrm{blank\ corr}} = \frac{\delta^{15}N_{\mathrm{sample}} \times \mathrm{area}_{\mathrm{sample}} - \delta^{15}N_{\mathrm{blank}} \times \mathrm{area}_{\mathrm{blank}}}{\mathrm{area}_{\mathrm{sample}} - \mathrm{area}_{\mathrm{blank}}} \quad (5)$$

where $\delta^{15}N_{\mathrm{blank\ corr}}$ is the $\delta^{15}N$ value of the samples after correction and $\delta^{15}N_{\mathrm{sample}}$ and $\delta^{15}N_{\mathrm{blank}}$ are the $\delta^{15}N$ values of samples and blanks directly measured by PT-IRMS. The $\mathrm{area}_{\mathrm{sample}}$ and $\mathrm{area}_{\mathrm{blank}}$ were also directly measured by PT-IRMS.

Samples collected from air and NO_x emission samples were evaporated to dryness in a water bath at 80 °C to remove the influence of H_2O_2 and filled with 5 mL deionized water before performing the ^{15}N-NO_3^- isotopic analysis.

Results and discussion

Precision of $\delta^{15}N$-NO_3^- analyses by chemical methods

The international $\delta^{15}N$-NO_3^- reference standards USGS34 and USGS32 were used to define the analytical precision. Standards for concentration analyses were produced in duplicate with 100 μmol L^{-1} solutions mixed together according to different volume ratios to generate distinct $\delta^{15}N$-NO_3^- compositions (Table 1). The mixed standard solutions and sample solutions were prepared from the same matrix to provide a comparable precision in the $\delta^{15}N$-NO_3^- results. There are good linear correlations between $\delta^{15}N$-NO_3^- values of standard solutions and measured $\delta^{15}N$-N_2O values of samples using the two methods (Fig. 3). The linear regression slopes for the cadmium–sodium azide and VCl_3–sodium azide methods were 0.45 and 0.44, respectively.

Table 1 Theoretical values of $\delta^{15}N$-NO_3^- in the standard solutions mixed by different volume ratios

No.	Volume ratio (V_A:V_B)	Theoretical value of $\delta^{15}N$-NO_3^- (‰)
1	6:0	− 1.8
2	5:1	28.5
3	4:2	58.8
4	3:3	89.1
5	2:4	119.4
6	1:5	149.7
7	0:6	180.0

V_A 100 μmol L^{-1} USGS34, V_B 100 μmol L^{-1} USGS32

In fact, the theory of reaction mechanisms reveals that the slope of the linear relation between the true $\delta^{15}N$ of a NO_3^- standard (or sample) and the measured $\delta^{15}N$ of the produced N_2O should to be 0.5, since one N atom in the N_2O product originates from NO_3^- and the other one from N_3^-. The intercept reflects the combination of the initial $\delta^{15}N$ of N_3^- values with the isotopic fractionation associated with the reactions from NO_3^- to N_2O.

In our study, the slopes of the regression lines were close to the 0.5 theoretical value predicted from the 1:1 mixture of NO_2^--N and N_3^--N. The correlation between concentration and signal intensity for NO_3^- reveals 3.8 nmol NO_3^- in the 5 mL blank samples (0.76 μmol L^{-1}), which was mainly derived from sodium azide in the VCl_3–sodium azide solution.

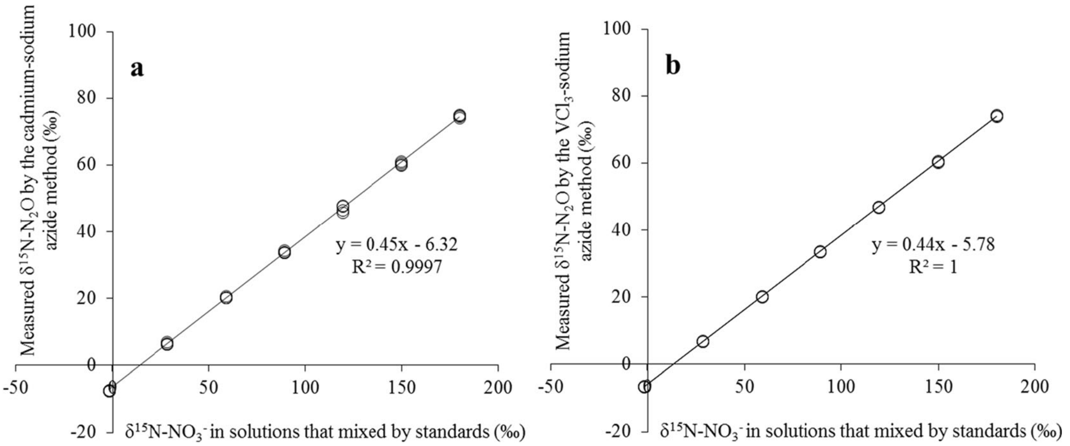

Fig. 3 Correlations between the $\delta^{15}N$-N_2O and the $\delta^{15}N$-NO_3^- in solutions mixed by standards

Furthermore, the correlation of the δ^{15}N-NO_3^- values in standard solutions with the measured δ^{15}N-N_2O values of samples also revealed the role of blank samples. Figure 4a shows an augmentation in the linear regression slope when the sample concentrations increased, whereas when the blank correction was applied through the mass balance equation, the slopes of the linear regression approached 0.5 (Fig. 4b).

Except for blanks, other effects such as the IRMS precision could be responsible for the results of measured δ^{15}N-NO_3^- values (Lachouani et al. 2010). However, the excellent correlation of standard and measured δ^{15}N demonstrated the methods to be robust and good quantitative techniques for measurement of δ^{15}N-NO_3^- in the environmental samples.

δ^{15}N-NO_3^- precision and accuracy

To evaluate the accuracy and precision of both methods of δ^{15}N isotopic analyses, we analyzed laboratory and international δ^{15}N-NO_3^- standards with each batch of submitted samples. Results showed that both methods presented accurate δ^{15}N-NO_3^- values defined by the international and in-lab standard numbers (Table 2). The δ^{15}N-NO_3^- standard deviations for the cadmium–sodium azide and the VCl_3–sodium azide methods were 0.34 and 0.33‰, respectively, which is excellent. Standards are important not only to assess the precision and accuracy of δ^{15}N-NO_3^- compositions and subsequent concentrations but also to determine the sample concentration limit of detection (LOD).

Throughout the course of this study, the blank NO_3^- concentration was 0.76 μmol L^{-1}, obtained by the VCl_3–sodium azide method. The LOD was determined by taking 10 times the NO_3^- concentrations of the blank (e.g., 7.6 μmol L^{-1}) in a 5 mL solution. The result produced an adequate accuracy and precision in the determination of the natural δ^{15}N-NO_3^-N from NO_x emissions from coal-fired power plants and motor vehicles, and low concentrations of gaseous NO_2 and HNO_3 (Table 3). The LOD value was much lower to that given by Lachouani et al. (2010).

The LOD associated with the cadmium–sodium azide method generated a PT-IRMS baseline signal intensity of *m/z* 44 corresponding to a concentration of 0.82 μmol L^{-1}. The accuracy and precision are acceptable when measuring the natural δ^{15}N-NO_3^- in surface water and soil extract samples and testing a LOD of 8.2 μmol L^{-1} through standards (Table 3).

Characterizations of δ^{15}N-NO_3^- values in different samples

Analytical results showed that the δ^{15}N-NO_3^- values of river water samples ranged from − 1.4 to 14.4‰, with a mean of 8.9 ± 3.3‰ (Fig. 5). This is comparable to the range of water δ^{15}N-NO_3^- values previously published in this region (Chen et al. 2012). However, our values were much higher relative to typical δ^{15}N-NO_3^- values taken at watershed outlets in predominantly forested land (Mayer et al. 2002). The variability in the δ^{15}N values of riverine NO_3^- could be sufficiently explained by mixing of NO_3^- from various sources. For example, river water originating from manure and sewage is much more enriched in ^{15}N relative to other N sources.

Soil extracts present an NO_3^- isotopic composition varying from − 4.3 to 8.6‰ (mean of 3.5 ± 3.5‰), which overlaps the range of typical soil δ^{15}N values

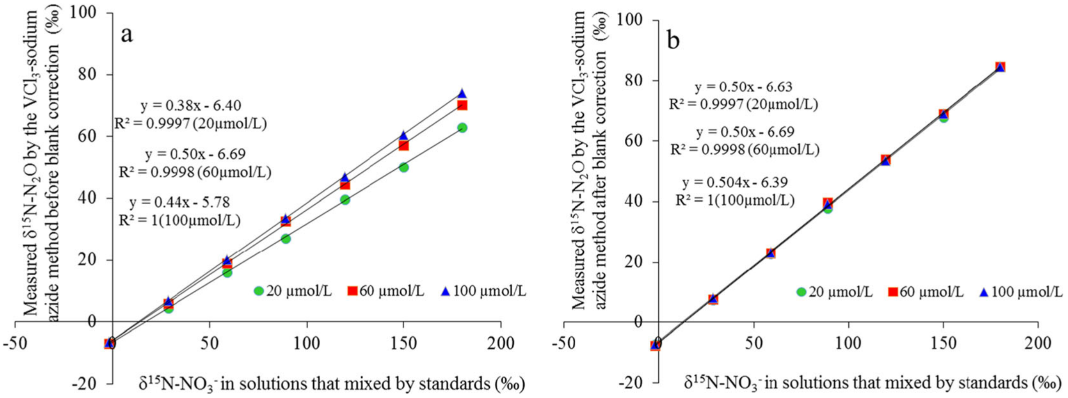

Fig. 4 Relationship between the δ^{15}N-N_2O and the δ^{15}N-NO_3^- in solutions mixed by standards before and after blank corrections of the VCl_3–sodium azide method

Table 2 $\delta^{15}N-NO_3^-$ values (‰) of international and lab standards and measured by PT-IRMS in this study

Standard	Reference value	Measured by the VCl_3–sodium azide method	Measured by the cadmium–sodium azide method
USGS-35	2.7 ± 0.2	2.78 ± 0.27 (*n* = 6)	2.93 ± 0.31 (*n* = 6)
IAEA-NO-3	4.7 ± 0.2	4.75 ± 0.20 (*n* = 6)	4.49 ± 0.34 (*n* = 6)
ST-1	3.7	3.65 ± 0.33 (*n* = 6)	3.82 ± 0.30 (*n* = 6)
ST-2	14.6	14.55 ± 0.31 (*n* = 6)	14.61 ± 0.29 (*n* = 6)

provided by Xue et al. (2009). The rate of mineralization and nitrification, soil depth, vegetation, climate, and site history may also affect the $\delta^{15}N$ composition in soil (Kendall 1998; Mayer et al. 2002).

The analyzed $\delta^{15}N-NO_3^-$ composition of summer rain water varied from − 4.6 to 9.5‰, with a mean of 3.3 ± 2.1‰ (Fig. 5). These values fall well within the range of previously reported values for atmospheric NO_3^- (Hastings et al. 2013; Elliott et al. 2007; Tobari et al. 2010; Russell et al. 1998), and are comparable to the results reported in southern China and in urban and suburban sites in the North China Plain (Fang et al. 2011). However, our results are higher than those for NO_3^- precipitates from two rural sites in the Hebei Province of northern China, and Japan, where most values of $\delta^{15}N-NO_3^-$ in rain water were negative(Fukuzaki and Hayasaka 2009). The higher values could result from higher contributions of NO_3^--N derived from vehicle exhausts and coal-fired boilers. For example, 33 sites across the mid-western and northeastern USA yielded $\delta^{15}N$ composition of wet NO_3^- depositions that ranged from − 8.1 to 3.2‰ with a mean value of − 1.5‰, and the highest $\delta^{15}N$ values in NO_3^- close to major stationary emission sources (Elliott et al. 2007).

The $\delta^{15}N-HNO_3$ values of representative emission sources are summarized in Fig. 5. Samples collected from coal-fired power plants yielded a mean $\delta^{15}N-NO_3^-$ value of 20.3 ± 4.3‰ with concentrations of HNO_3 ranging from 60 to 80 mg m^{-3}, close to the mean value of coal fire reported by Felix et al. (2012). The $\delta^{15}N-NO_3^-$ values of vehicular emissions collected in this study ranged from 0.4 to 9.4‰, with a mean of 5.7 ± 3.6‰. The range and standard deviation of $\delta^{15}N-NO_3^-$ of the vehicle emissions in this study are lower than those published by Felix and Elliott (2014). The values are also higher than the values obtained from 26 gasoline and diesel-powered vehicles controlled by the NO_2/NO_x molar ratios (Walters et al. 2015)

Gaseous HNO_3 measurements produced concentrations with a range of 1.71–16.07 μg N m^{-3} during the summer. The $\delta^{15}N-HNO_3$ values varied from 2.2 to 10.8‰, with a mean value of 5.9 ± 2.4‰, higher than that of other studies. For example, in Ohio, New York, and Pennsylvania, 96 measurements of gaseous $\delta^{15}N-HNO_3$ ranged from − 4.9 to 10.8‰ with a mean of 3.2‰ (Elliott et al. 2009). In addition, a study on variation of gaseous $\delta^{15}N-NO_3^-$ values at Akita in Japan was even lower than 0‰ (Kawashima 2014). Concentrations of HNO_3 are also correlated with stationary source emissions, suggesting that the spatial distribution of stationary sources is a primary control on HNO_3 formation and associated $\delta^{15}N-HNO_3$ values (Elliott et al. 2009).

Isotopes as tracers of anthropogenic NO_3^--N sources and impacts

Excess N causes environmental pollution and threatens agricultural productivity, food security, ecosystem and

Table 3 Precision and accuracy of limit of detection (LOD) for N isotope analysis in this study (the LOD was 8.2 and 7.6 μmol L^{-1} for the cadmium–sodium azide method and VCl_3–sodium azide method, respectively)

Standard	Reference value	Measured by the VCl_3–sodium azide method	Measured by the cadmium–sodium azide method
USGS-35	2.7 ± 0.2	2.63 ± 0.47 (*n* = 6)	2.61 ± 0.57 (*n* = 6)
IAEA-NO-3	4.7 ± 0.2	4.78 ± 0.55 (*n* = 6)	4.75 ± 0.65 (*n* = 6)
ST-1	3.7	3.87 ± 0.51 (*n* = 6)	3.85 ± 0.77 (*n* = 6)
ST-2	14.6	14.49 ± 0.49 (*n* = 6)	14.53 ± 0.82 (*n* = 6)

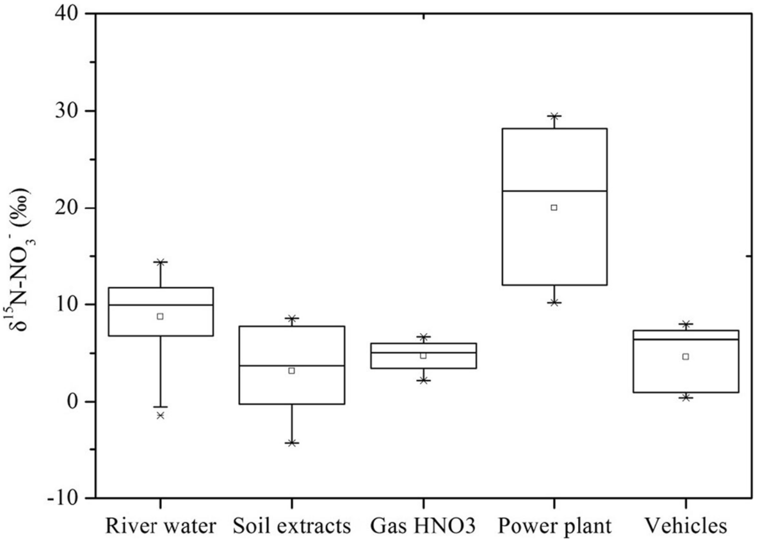

Fig. 5 δ^{15}N-NO_3^- values of major N cycle processes in this study. The rectangular boxes indicate the interquartile range (first and third quartiles), median values are indicated by the centerline within each box, and outliers are indicated by circles

human health, and economic prosperity (Zhang et al. 2015). The isotopic composition of NO_3^- is not only a powerful tool to determine its origin but can also provide clues about the N transformation processes such as NH_3 volatilization and denitrification (Mayer et al. 2002). Furthermore, stable isotopes contained in reactive N compounds are providing new insights into the environmental N cascade, since N sources present different stable isotope signatures that can be used to assess the N flow (Hastings et al. 2013).

Isotopic studies have helped determine the source, origin, and cycle of N. The δ^{15}N-NO_3^- composition confirmed that the source of NO_3^- deposited across the northeastern USA came principally from power plant NO_x emissions (Elliott et al. 2007; Felix et al. 2012). The isotopic composition of NO_3^-, combined with $\Delta^{17}NO_3$ and $\delta^{18}NO_3$ values, established the main terrestrial sources of NO_3^- to be the sewage and manure effluents in the upstream areas of the Yellow River in China (Liu et al. 2013).

The sources of N carry distinct stable isotope signatures. The δ^{15}N-NO_3^- analysis of water and air samples in this study showed that the measured δ^{15}N-NO_3^- values of coal-fired power plants were much higher than those other power plants (Fig. 5). The δ^{15}N-NO_3^- data demonstrated that NO_x emitted from motor vehicles and soil extracts has relatively low δ^{15}N values. Although various processes such as fractionation and seasonality of oxidation pathways can influence the isotopic values of N compounds, the range of δ^{15}N-NO_3^- values coming from motor vehicle samples was close to that of gaseous HNO_3, and thus, motor vehicle emissions can be considered the major source of gaseous HNO_3.

Conclusions

The cadmium–sodium azide and the VCl_3–sodium azide chemical methods were successfully used to determine the δ^{15}N-NO_3^- composition of samples with low N concentration, small N volume, and complex absorbing solutions based on the conversion of NO_3^- into N_2O, analyzed by PT-IRMS. The good linear correlation of measured δ^{15}N values between standard and sample demonstrated the soundness of both chemical methods and of the quantitative measurement technique for δ^{15}N-NO_3^-. The low standard deviations provided by the δ^{15}N-NO_3^- values indicated excellent precision. The sample concentration LOD obtained by the VCl_3–sodium azide and cadmium–sodium azide methods were 7.6 and 8.2 μmol L^{-1}, respectively.

Results indicated that river water samples collected in this study showed a δ^{15}N-NO_3^- value from − 1.4 to 14.4‰ with a mean of 8.9 ± 3.3‰. The δ^{15}N-NO_3 of soil extracts varied from − 4.3 to 8.6‰, with a mean of 3.5 ± 3.5‰. The analyzed δ^{15}N-NO_3^- values in summer rain water samples varied from − 4.6 to 9.5‰. The δ^{15}N values of HNO_3 sampled from coal-fired power plants display a mean value of 20.3 ± 4.3‰, and δ^{15}N-NO_3^- values of motor vehicle emissions collected in a tunnel ranged from 0.4 to 9.4‰ with a mean of 5.7 ± 3.6‰. Measurements of gaseous HNO_3

yielded δ^{15}N-NO_3^- values ranging from 2.2 to 10.8‰, with a mean of 5.9 ± 2.4‰.

In summary, the NO_x emitted from motor vehicles and soil extracts exhibited relatively low δ^{15}N values, whereas the vehicle values were close to those of gaseous HNO_3. The isotopic signatures presented in this study can be used to identify and trace the transport of N.

Acknowledgements This study was supported by the Key Research Program of the Chinese Academy of Sciences (Grant No. ZDRW-ZS-2016-5-1), the Natural Science Foundation of Jiangsu Province (Grant No. BK20131047), and the National Natural Science Foundation of China (Grant No. 41301578).

Compliance with ethical standards

Conflict of interest The authors declare that they have no conflict of interest.

References

Adon, M., Galy-Lacaux, C., Yoboue, V., Delon, C., Lacaux, J. P., Castera, P., et al. (2010). Long term measurements of sulfur dioxide, nitrogen dioxide, ammonia, nitric acid and ozone in Africa using passive samplers. *Atmospheric Chemistry and Physics, 10*(15), 7467–7487. https://doi.org/10.5194/acp-10-7467-2010.

Braman, R. S., & Hendrix, S. A. (1989). Nanogram nitrite and nitrate determination in environmental and biological-materials by vanadium(Iii) reduction with chemiluminescence detection. *Analytical Chemistry, 61*(24), 2715–2718. https://doi.org/10.1021/ac00199a007.

Casciotti, K. L., Sigman, D. M., Hastings, M. G., Bohlke, J. K., & Hilkert, A. (2002). Measurement of the oxygen isotopic composition of nitrate in seawater and freshwater using the denitrifier method. *Analytical Chemistry, 74*(19), 4905–4912. https://doi.org/10.1021/ac020113w.

Chen, Z. X., Liu, G., Liu, W. G., Lam, M. H. W., Liu, G. J., & Yin, X. B. (2012). Identification of nitrate sources in Taihu Lake and its major inflow rivers in China, using δ^{15}N-NO_3^- and δ^{18}O-NO_3^- values. *Water Science and Technology, 66*(3), 536–542. https://doi.org/10.2166/wst.2012.193.

Elliott, E. M., Kendall, C., Boyer, E. W., Burns, D. A., Lear, G. G., Golden, H. E., et al. (2009). Dual nitrate isotopes in dry deposition: Utility for partitioning NO_x source contributions to landscape nitrogen deposition. *Journal of Geophysical Research-Biogeosciences, 114*, doi:Artn G04020https://doi.org/10.1029/2008jg000889.

Elliott, E. M., Kendall, C., Wankel, S. D., Burns, D. A., Boyer, E. W., Harlin, K., Bain, D. J., & Butler, T. J. (2007). Nitrogen isotopes as indicators of NO_x source contributions to atmospheric nitrate deposition across the Midwestern and northeastern United States. *Environmental Science & Technology, 41*(22), 7661–7667. https://doi.org/10.1021/es070898t.

Erisman, J. W., Galloway, J. N., Seitzinger, S., Bleeker, A., Dise, N. B., Petrescu, A. M. R., Leach, A. M., & de Vries, W. (2013). Consequences of human modification of the global nitrogen cycle. *Philosophical Transactions of the Royal Society B-Biological Sciences, 368*(1621), 20130116. https://doi.org/10.1098/rstb.2013.0116.

Fang, Y. T., Koba, K., Wang, X. M., Wen, D. Z., Li, J., Takebayashi, Y., Liu, X. Y., & Yoh, M. (2011). Anthropogenic imprints on nitrogen and oxygen isotopic composition of precipitation nitrate in a nitrogen-polluted city in southern China. *Atmospheric Chemistry and Physics, 11*(3), 1313–1325. https://doi.org/10.5194/acp-11-1313-2011.

Felix, J. D., & Elliott, E. M. (2014). Isotopic composition of passively collected nitrogen dioxide emissions: Vehicle, soil and livestock source signatures. *Atmospheric Environment, 92*, 359–366. https://doi.org/10.1016/j.atmosenv.2014.04.005.

Felix, J. D., Elliott, E. M., & Shaw, S. L. (2012). Nitrogen isotopic composition of coal-fired power plant NO_x: Influence of emission controls and implications for global emission inventories. *Environmental Science & Technology, 46*(6), 3528–3535. https://doi.org/10.1021/es203355v.

Freyer, H. D. (1978). Seasonal trends of NH_4^+ and NO_3- nitrogen isotope composition in rain collected at Julich, Germany. *Tellus, 30*(1), 83–92. https://doi.org/10.1111/j.2153-3490.1978.tb00820.x.

Fukuzaki, N., & Hayasaka, H. (2009). Seasonal variations of nitrogen isotopic ratios of ammonium and nitrate in precipitations collected in the Yahiko-Kakuda mountains area in Niigata prefecture, Japan. *Water Air and Soil Pollution, 203*(1–4), 391–397. https://doi.org/10.1007/s11270-009-0026-8.

Hastings, M. G., Casciotti, K. L., & Elliott, E. M. (2013). Stable isotopes as tracers of anthropogenic nitrogen sources, deposition, and impacts. *Elements, 9*(5), 339–344. https://doi.org/10.2113/gselements.9.5.339.

Kawashima, H. (2014). Formation mechanism and source apportionment of ammonium and nitrate ions in aerosol using nitrogen isotopes. *Earozoru Kenkyu, 29*(s1), 110–116.

Kendall, C. (1998). Tracing sources and cycling of nitrate in catchments. In C. Kendall & J. J. McDonnell (Eds.), *Isotope tracers in catchment hydrology* (pp. 519–576). Amsterdam: Elsevier.

Kendall, C., Elliott, E. M., & Wankel, S. D. (2007). Tracing anthropogenic inputs of nitrogen to ecosystems. *Stable Isotopes in Ecology and Environmental Science, 2nd Edition*, 375–449, doi:DOI https://doi.org/10.1002/9780470691854.ch12.

Lachouani, P., Frank, A. H., & Wanek, W. (2010). A suite of sensitive chemical methods to determine the δ^{15}N of ammonium, nitrate and total dissolved N in soil extracts. *Rapid Communications in Mass Spectrometry, 24*(24), 3615–3623. https://doi.org/10.1002/rcm.4798.

Liu, T., Wang, F., Michalski, G., Xia, X. H., & Liu, S. D. (2013). Using ^{15}N, ^{17}O, and ^{18}O to determine nitrate sources in the Yellow River, China. *Environmental Science & Technology, 47*(23), 13412–13421. https://doi.org/10.1021/es403357m.

Mayer, B., Boyer, E. W., Goodale, C., Jaworski, N. A., Van Breemen, N., Howarth, R. W., et al. (2002). Sources of nitrate in rivers draining sixteen watersheds in the northeastern US:

Isotopic constraints. *Biogeochemistry, 57*(1), 171–197. https://doi.org/10.1023/A:1015744002496.

McIlvin, M. R., & Altabet, M. A. (2005). Chemical conversion of nitrate and nitrite to nitrous oxide for nitrogen and oxygen isotopic analysis in freshwater and seawater. *Analytical Chemistry, 77*(17), 5589–5595. https://doi.org/10.1021/ac050528s.

Michalski, G., Meixner, T., Fenn, M., Hernandez, L., Sirulnik, A., Allen, E., & Thiemens, M. (2004). Tracing atmospheric nitrate deposition in a complex semiarid ecosystem using $\Delta^{17}O$. *Environmental Science & Technology, 38*(7), 2175–2181. https://doi.org/10.1021/es034980+.

Rock, L., & Ellen, B. H. (2007). Nitrogen-15 and oxygen-18 natural abundance of potassium chloride extractable soil nitrate using the denitrifier method. *Soil Science Society of America Journal, 71*(2), 355–361. https://doi.org/10.2136/sssaj2006.0266.

Russell, K. M., Galloway, J. N., Macko, S. A., Moody, J. L., & Scudlark, J. R. (1998). Sources of nitrogen in wet deposition to the Chesapeake Bay region. *Atmospheric Environmental, 32*(14–15), 2453–2465. https://doi.org/10.1016/S1352-2310(98)00044-2.

Schilman, B., & Teplyakov, N. (2007). Detailed protocol for nitrate chemical reduction to nitrous oxide for δ15N and δ18O analysis of nitrate in fresh and marine waters. *Annual Report Submitted to the Earth Science Research Administration, Ministry of National Infrastructures Jerusalem, December 2007*.

Sigman, D. M., Casciotti, K. L., Andreani, M., Barford, C., Galanter, M., & Bohlke, J. K. (2001). A bacterial method for the nitrogen isotopic analysis of nitrate in seawater and freshwater. *Analytical Chemistry, 73*(17), 4145–4153. https://doi.org/10.1021/ac010088e.

Silva, S. R., Kendall, C., Wilkison, D. H., Ziegler, A. C., Chang, C. C. Y., & Avanzino, R. J. (2000). A new method for collection of nitrate from fresh water and the analysis of nitrogen and oxygen isotope ratios. *J Hydrology, 228*(1–2), 22–36. https://doi.org/10.1016/S0022-1694(99)00205-X.

Stedman, G. (1959a). Mechanism of the Azide-Nitrite Reaction .1. *Journal of the Chemical Society*(Sep-O), 2943–2949, doi: DOI https://doi.org/10.1039/jr9590002943.

Stedman, G. (1959b). Mechanism of the Azide-Nitrite Reaction .2. *Journal of the Chemical Society*(Sep-O), 2949–2954, doi: DOI https://doi.org/10.1039/jr9590002949.

Tobari, Y., Koba, K., Fukushima, K., Tokuchi, N., Ohte, N., Tateno, R., Toyoda, S., Yoshioka, T., & Yoshida, N. (2010). Contribution of atmospheric nitrate to stream-water nitrate in Japanese coniferous forests revealed by the oxygen isotope ratio of nitrate. *Rapid Communications in Mass Spectrometry, 24*(9), 1281–1286. https://doi.org/10.1002/rcm.4498.

Tsunogai, U., Kido, T., Hirota, A., Ohkubo, S. B., Komatsu, D. D., & Nakagawa, F. (2008). Sensitive determinations of stable nitrogen isotopic composition of organic nitrogen through chemical conversion into N2O. *Rapid Communications in Mass Spectrometry, 22*(3), 345–354. https://doi.org/10.1002/rcm.3368.

Walters, W. W., Goodwin, S. R., & Michalski, G. (2015). Nitrogen stable isotope composition ($\delta^{15}N$) of vehicle-emitted NO_x. *Environmental Science & Technology, 49*(4), 2278–2285. https://doi.org/10.1021/es505580v.

Xue, D. M., Botte, J., De Baets, B., Accoe, F., Nestler, A., Taylor, P., et al. (2009). Present limitations and future prospects of stable isotope methods for nitrate source identification in surface- and groundwater. *Water Research, 43*(5), 1159–1170. https://doi.org/10.1016/j.watres.2008.12.048.

Xue, D. M., De Baets, B., Botte, J., Vermeulen, J., Van Cleemput, O., & Boeckx, P. (2010). Comparison of the silver nitrate and bacterial denitrification methods for the determination of nitrogen and oxygen isotope ratios of nitrate in surface water. *Rapid Communications in Mass Spectrometry, 24*(6), 833–840. https://doi.org/10.1002/rcm.4445.

Zhang, X., Davidson, E. A., Mauzerall, D. L., Searchinger, T. D., Dumas, P., & Shen, Y. (2015). Managing nitrogen for sustainable development. *Nature, 528*(7580), 51–59. https://doi.org/10.1038/nature15743.